Z-H BOOST CONVERTER FOR DC MICROGRIDS – MODELLING AND SIMULATION

[1]Ch.Sajan, [2]T.Praveen kumar, [3]Ch.Akhil, [4]K.Shivakumar

[1]Associate professor, [2]Associate professor, [3]Student Member, [4]Student Member
[1]Department of Electrical and Electronics Engineering,
[1] Jyothishmathi Institute of Technology and Science, Karimnagar, India

Abstract: With the scarcity of the energy and ever rising of the oil price, research on the renewable and green energy sources, exclusively the solar arrays and the fuel cells, becomes more and more vital. Boost converters are universally used to attain high step-up and high efficiency DC/DC converters and also used as power-factor corrected preregulators. A Z-H Boost dc-dc converter is proposed in this paper as there's no shoot-through switching state in this converter and the front end diode is wiped out. The Z-H Boost Converter can be adapted to dc-dc, dc-ac, ac-dc, and ac-ac power conversion. The simulation results verified the analysis and demonstrated the tremendous potential of the Z-H Boost converter.

IndexTerms **- Boost Converters, Photovoltaic module, Z-H Boost Converter, Power Losses**

I. INTRODUCTION

In the world's energy portfolio, Photovoltaic (PV) sources are one of the important competitor and will become the enormous contributions to the electricity generation among all renewable energy changellers by the year 2040 because it is absolutely clean, emission-free renewable electrical generation technology with high reliability. Boost converters are the most oustanding, especially for applications with dc bus voltage much higher than line input. These are generally applied as preregulators or even combined with the latter-stage circuits or rectifiers into single-stage circuits [1]-[2]. The easiness in circuit and system design, reduced voltage stress on devices and high conversion, high-power-factor concern are the reasons for using boost converter. The conventional method of reducing input current harmonics using an *LC* input filter is no longer practically bearable to meet the requirements in many high-power applications.

Most renewable power sources, such as photovoltaic power systems and fuel cells, have quite low-voltage output and requires a voltage booster to provide sufficient voltage output [3], [4]. However, there are some impediments for the conventional interleaved boost converter in high step-up DC/DC conversion.

1) The current ripples of the switches and the output diodes are large.
2) The switch voltage stress is equal to the output voltage, which is large in high output voltage applications.
3) The switching losses and the output diode reverse-recovery losses are large due to the hard switching operation and high switch voltage stress.

This paper presents an impedance source network that can be used for the high voltage gain with small duty cycle ratio, which reduces the voltage stress of components and also reduces the switching losses.

II. MODELLING OF PV MODULE

The system structure of the prospective DC microgrid consists of a common radial DC bus of 200V, to which the different parts of the microgrid are connected. Solar PV is treated as the primary source of power in this configuration. A solar PV array is connected to the microgrid using a boost converter. The microgrid system supplies a variable DC load, which can be in the form of a collection of houses or a building load. The configuration of the DC microgrid is designed in such a way that it can operate individually without any connection to the utility. The single diode model or the five parameter model [7] is used for modelling the solar cell.

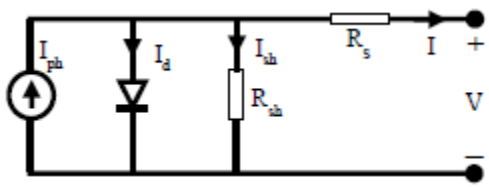

fig. 1. equivalent circuit of a pv cell

The equivalent circuit of a solar PV cell is given in Fig. 1. It consists of a current source, a diode, a series resistance and a parallel resistance. The current source represents the photo current (I_{ph}) produced inside the PV cell which is a function of the incident solar radiation (G) and cell temperature (T). The current I_d is the diode current and I_{sh} represents the current in the shunt branch. R_{sh} and R_s are the shunt and series resistances. V and I represent the output voltage and current from the cell. Employing Kirchhoff's law, the equation of the current can be written as,

$$I = I_{ph} - I_d - I_{sh} \quad (1)$$

The diode current (I_d) and the shunt current (I_{sh}) is given by the following.

$$I_d = I_s \{\exp [(V+IRs)/nCKT] - 1\} \quad (2)$$

$$I_{sh} = [V+IRs]/Rsh \quad (3)$$

Where q is the electric charge (1.6×10-19 C), K is the
Boltzmann constant (1.38×10-23 J/K), C is the number of cells in a PV module, T is the cell temperature (K) and n is the diode ideality factor. In order to reduce complication, it is assumed that only photo current and the diode current depends on the working conditions [7]. The dependencies are specified by the Townsend equations which are given as,

$$I_{ph} = [G/Gref][I_{sc} + \mu_{sc}(T - T_{ref})] \quad (4)$$

$$I_s = I_{s,\,ref}\,[T/T_{ref}]^3 * \exp\{qEgNs/nK(1/T - 1/T_{ref})\} \quad (5)$$

Where G is the incident solar irradiation, G_{ref} is the reference solar irradiation (taken as 1000 w/m^2), μ_{sc} is the temperature coefficient of the short circuit current and E_g is the band gap energy of the PV cell. The value of the reference diode saturation current is given by,

$$I_{s,} = I_{sc} / \{\exp(qV_{oc}/nCKT) - 1\} \quad (6)$$

Where, V_{oc} is the open circuit voltage across the PV module created by connecting a string of PV cells arranged in order to produce the required voltage and current output. For a individual reference operating condition, the values of the series resistance, parallel resistance and diode ideality factor are determined and these values are used for other conditions. Certainly, a model of a solar PV module is constructed using (1) - (6) Simulink.

For the simulation of the DC microgrid, a PV array is used. This array is connected to the DC distribution system via a boost converter. Here the boost converter employees the Maximum Power Point Tracking (MPPT). This feature of MPPT is a must as it will allow the PV array to deliver the maximum possible power for a particular irradiation input.

III. Z-H BOOST CONVERTER DESIGN AND THEORY OF OPERATION

A Modern dc-dc converter topology called a Z-H boost converter inspired from a Z-source inverter is presented in [5] by eliminating the front-end diode as shown in Fig. The output has four ports connected to an H-bridge where as the input of the impedance network has two ports connected to the power source. The perception of using the shoot-through duty cycle to regulate the output voltage is eliminated completely by simple control of the duty cycle of the switches. The gain of the converter is similar to that of the Z-source network but it can obtain two-quadrant operation modes (II & IV quadrant) by varying the duty cycle of the reciprocal switch in the D=[0,0.5] with positive output voltage and boost mode in D=[0.5,1] with negative output voltage range respectively.

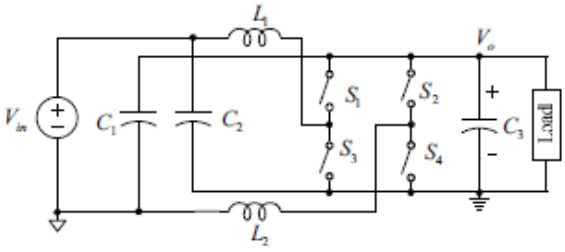

fig. 2. z-h boost converter with load

Z-H boost converter is similar to the Z-source, this proposed topology can be applied to dc-dc, dc-ac, ac-dc or ac-ac power conversion. The two middle points of the H-bridge are connected to the two inductors respectively.

The Z-H boost converter shown in Fig. 2. is a voltage-source converter which means there's no shoot-through switching state anymore. All the switches shown in Fig. 2. are bidirectional S_1 and S_3, S_2 and S_4 are achieved respectively.The control signals for S_2 and S_3 can be in phase, or have 180 phase shift to lower the voltage ripples. The sequence of gate signals is shown in Fig. 3. Here, D is the duty cycle for S_2 and S_3. The converter has two operating states: current charging state (T_0) and current discharging state (T_1).

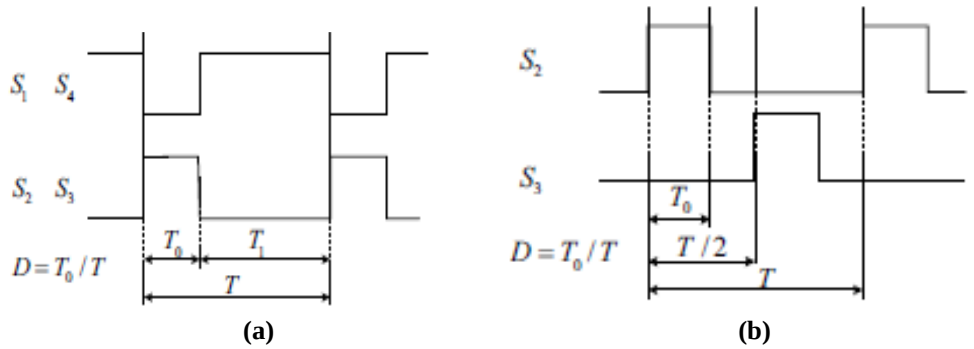

fig. 3. the sequence of gate signals. (a). s_2 and s_3 are in phase .(b). s_2 and s_3 are interleaved.

In order to generate the switching signals, a triangular carrier wave is compared to a constant reference signal. If the triangular carrier wave exceeds the reference signal, the switches S_1 and S_4 are turned on and S_2 and S_3 are turned off and vice versa. Boost Factor is given as: B = [1-2D]-1

where,

$0 \leq D \leq 0.5$ for Vo > 0 and $0.5 \leq D \leq 1$ for Vo < 0

Voltage Stress on the Switching Device is given as: $[1/1\text{-}2D]V_{in}$

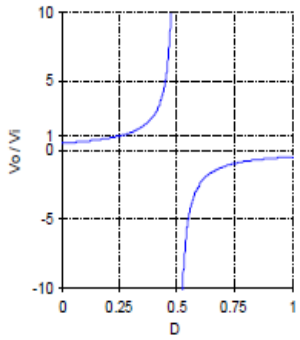

fig. 4. variation of voltage gain versus duty cycle for the z-h converter.

IV. CALCULATION OF POWER LOSSES AND THERMAL PERFORMANCE

(a) Switching and conduction losses calculations:

When the device is transitioning from the blocking state to the conducting state and vice-versa switching losses occurs. This period is described by a significant voltage across its terminals and a significant current through it.

Each transition needs to be multiplied by the switching frequency to obtain the switching losses for the energy dissipation. The switching losses P_{sw} are expressed as:

$$P_{sw} = (E_{on} + E_{off}) \times f_{sw} \quad (7)$$

where E_{on} and E_{off} are the energy losses during turn on and turn off of the switch, f_{sw} is the switching frequency. During the device is in full conduction mode, conduction losses occurs.

These losses are in direct relationship with the duty cycle. The average conduction losses P_{cond} are expressed as:

$$P_{avg.cond} = 1/T\int_0^T [vce(t) \times ice(t)]\, dt \quad (8)$$

Where v_{ce} is the on state voltage, an i_{ce} is the on state current. The time period T is as given as:

$$T = 1/f_{sw} \quad (9)$$

where f_{sw} is inversely proportioinal to T.

(b) Capacitor ESR losses calculations:

An ideal capacitors and inductors in series with a resistance, this resistance is defined as the equivalent series resistance (ESR). The value of the resistance is equal to the total effect of a large set of energy loss mechanisms occurring under the operating conditions. In a good capacitor, the ESR is very small, and in a poor capacitor the ESR is large. However, the ESR is not simply the resistance that would be measured across a capacitor by an ohmmeter, the ESR is a derived quantity with physical origins in both the dielectric's conduction electrons and dipole relaxation phenomena. The capacitors losses are expressed as:

$$P_{cap.loss} = I^2_{cap} \times ESR \quad (10)$$

(c) Magnetic core design calculations:

High Flux cores offer the highest biasing capability of all powder core materials. The high saturation flux density (15,000 gauss) and relatively low losses of High Flux cores make them quite useful for applications involving high power, high DC bias.

In this section, the magnetic core design is illustrated through the following steps:

1) In order to select a proper core size, the DC current and the inductance required with DC bias should be known from the core selector chart according to the calculated value in (11).

$$LI_{DC}{}^{2} \Rightarrow (mH.A^{2}) \quad (11)$$

A high flux 58337 core, was selected for the Z-H Boost converter in order to have fair comparison from an efficiency point of view.

2) Inductance, core size and permeability are now known, then calculating the no. of turns by determine the minimum inductance factor A_{Lmin} by using the unconditional negative tolerance (generally −8%) given in the core data sheet in (12) and (13)

$$A_{lmin} = A_l - 0.08Al \quad (12)$$

$$N = \sqrt{(L \times 10^{3})}/\sqrt{A_{lmin}} \quad (13)$$

Where A_{lmin} is the minimum inductance factor (nH/T^2), and L is the inductance in (μH).

3) The DC resistance can be estimated after knowing the winding factor of the core, wire gauge (AWG), and the no. of turns. The DC resistance can be calculated in (14) as:

$$R_{DC} = MLT \times N \times \Omega/Length \quad (14)$$

Where, MLT is the mean length per turn, and Ω/Length is the resistance per meter.

V. SIMULATION MODEL AND RESULTS

The Z-H boost converter has the capability of ideally giving an output voltage range from zero to infinity regardless of the input voltage. This utility of the Z-H boost converter for DC microgrid applications exhibits the superior suitability. The parameters of the impedance source network is chosen as L1=L2=0.4mH and C1=C2=C3=97μF. Switching frequency used in the simulation is 20kHz. The simulation parameters is given in table. I. and simulation results for Z-H boost converter are shown in figures (6),(7).

table I
specifications of simulation model

Simulation Parameters	Values
Power rating	3kw
Sampling frequency, f_s	20kHz
Output Voltage, V_o	200V
Voltage ripple	2-5%
Input Voltage,V_{in}	48V
Constant PV Array, V_{in}	Irradiance: 1000W/m^2 Temperature: 30°C

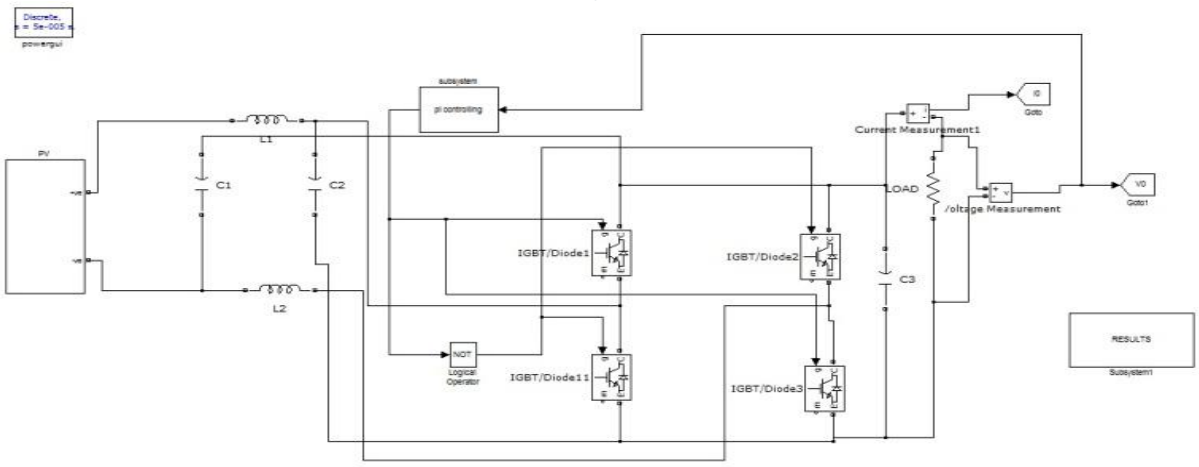

fig. 5. simulink model of the z-h boost converter with pv source for dc microgrids

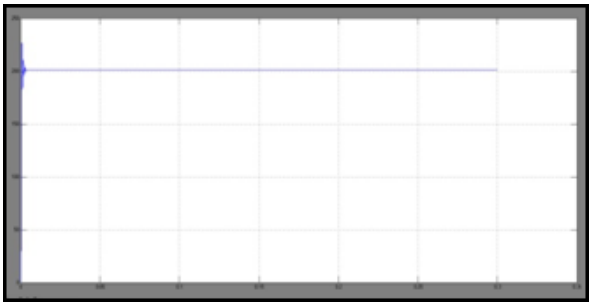

fig. 6. output voltage waveform of pv based boost converter under steadystate for 1000w/m^2 irradiance

fig. 7. output current waveform of pv based boost converter under steadystate for 1000w/m^2 irradiance

VI. CONCLUSION

This paper has confered the performance and suitability of a Z-H source boost DC-DC converter for DC microgrid applications. PV system with power electronic interface is modelled using MATLAB/Simulink circumstances. The PI controller furnishes a controlled output voltage for variable operating conditions of the PV source. It can be observed that the operating conditions of the Z-H boost DC-DC converter bids better performance and efficiency.

REFERENCES

[1] C. M.Wang, "A new single-phase ZCS-PWM boost rectifier with high power factor and low conduction losses," IEEE Trans. Ind. Electron., vol. 53, no. 2, pp. 500–510, Apr. 2006.

[2] K. P. Louganski and J. S. Lai, "Current phase lead compensation in single-phase PFC boost converters with a reduced switching frequency to line frequency ratio," IEEE Trans. Power Electron., vol. 22 , no. 1, pp. 113–119, Jan. 2007.

[3] K. Kobayashi, H. Matsuo, and Y. Sekine, "Novel solar-cell power supply system using a multiple-input DC–DC converter," IEEE Trans. Ind. Electron., vol. 53, no. 1, pp. 281–286, Feb. 2006.

[4] S. K. Mazumder , R. K. Burra, and K. Acharya, "A ripple-mitigating and energy-efficient fuel cell power-conditioning system," IEEE Trans. Power Electron. , vol. 22, no. 4, pp. 1437–1452, Jul. 2007.

[5] F. Zhang, F. Z. Peng and Z. Qian, "Z-H Converter," in Proc. PESC 2008, pp. 1004-1007, June 2008.

[6] F. Z. Peng, M. Shen and Z. Qian, "Maximum Boost Control of the Z-Source Inverter," IEEE Trans. Power Electron., vol. 20, no. 4, pp. 833-838, July 2005.

[7] F. Evran and M. T. Aydemir, "Isolated high step-up DC-DC converter with low voltage stress", IEEE Trans. Power Electron, (early access-2013).

[8] R.T. Naayagi, A.J. Forsyth, R. Shuttleworth, "High-Power Bidirectional DC-DC Converter for Aerospace Applications," IEEE Transactions on Power Electronics, vol. 27, no. 11, pp. 4366-4379, November 2012.

[9] W. Li, X. He, "Review of non-isolated high-step-up dc/dc converters in photovoltaic grid-connected applications," IEEE Transactions on Industrial Electronics, vol.58, no.4, pp.1239–1250, April 2011.

[10] Y. Tang, X. Dong, and Y. He, "Active buck-boost inverter," IEEE Trans.Ind. Electron., vol. 61, no. 9, pp. 4691–4697, Sep. 2014.

[11] N. V. Nguyen, B. X. Nguyen, and H. H. Lee, "An optimized discontinuous PWM method to minimize switching loss for multilevel inverters," IEEE Trans. Ind. Electron., vol. 58, no. 9, pp. 3958 -3966, Sep. 2011.

[12] K. Ramtek and Y. N. and, "Dynamic modeling and controller design for z-source dc-dc converter," International Journal of Scientific Engineering and Technology, vol. 2, no. 4, pp. 272–277, Apr. 2013.

[13] Wuhua Li, Xiaodong Lv, Yan Deng, Jun Liu, Xiangning He "A Review of Non-Isolated High Step-Up DC/DC Converters in Renewable Energy Applications" IEEE Trans. Power Electron, pp. 978-1-422-2812-0/09, 2009.